Available online at www.sciencedirect.com
SCIENCE DIRECT®
Journal of Sound and Vibration 263 (2003) 451–466
JOURNAL OF SOUND AND VIBRATION
www.elsevier.com/locate/jsvi

Letter to the Editor

On the forced harmonic response of a flexible disc rotating near a rigid wall

A.K. Bajaj*, G. Naganathan, S. Ramadhyani

School of Mechanical Engineering, Purdue University, 1288 Mechanical Engineering Building, West Lafayette, IN 47907-1288, USA

Received 23 September 2002; accepted 2 October 2002

1. Introduction

The dynamics of a flexible spinning disk is a topic of great current interest. Spinning disks are encountered in computer memory disks, circular saw blades, turbine rotors, rotor disks and other machine elements. The ever increasing need for higher spin rate to reduce the access time for reading/writing of data in a computer memory disk calls for high-reliability and high-speed disks. In computer applications, the hard/floppy disk rotates very close to a base plate. The thin air film between the disk and the base plate helps to stabilize the transverse vibrations of the disk, allowing the disk to be operated at high rotation speeds. Disks stabilized by this technique are commonly used for data storage and are called *Bernoulli* disks. For disks spinning at high speeds near a rigid plate on a thin air film, there is a potential danger for the disks to undergo self-excited oscillations resulting from the coupling between the dynamics of the disk and the hydrodynamics of the film. When the self-excited instability arises, the amplitude of the disk vibration increases even in the absence of any external force. The effect of an external load on a spinning disk is also frequently encountered in magnetic recording applications by way of a read/write head and in spinning saw blade applications by way of work piece load.

One of the earliest investigations into the vibrations of a spinning disk was conducted by Lamb and Southwell [1]. They derived the linearized equations for transverse deflection of the disk and identified contributions from the bending and the in-plane stresses due to rotation. They also examined the frequencies and modes of free vibration for very flexible and very rigid disks. Southwell [2] investigated the effects of a central clamp on the natural frequencies of the spinning disk system while including flexural rigidity as well as membrane stresses. Prescott [3] later extended the analysis to disks with different clamping geometries and cross-sections. Simmonds [4] studied the transverse vibrations of a flat centrally clamped spinning membrane, ignoring the

*Corresponding author. Fax: +765-494-0539.
E-mail address: bajaj@ecn.purdue.edu (A.K. Bajaj).

0022-460X/03/$ - see front matter
doi:10.1016/S0022-460X(02)01467-0

bending stresses. Eversman and Dodson [5] included bending rigidity along with membrane stresses and obtained the solution of the linear problem by using a power series expansion, and by using a perturbation expansion about a singular point. The frequencies of vibration were obtained as a function of the ratio of the clamping radius to the outer radius.

Research into the effects of the fluid medium on the transverse vibrations of rotating disks was started by Pearson [6]. His work involved experimental investigation of a disk spinning in close proximity of a base plate. His experiments showed that the presence of a base plate stabilizes the transverse motion of the disk. Pelech and Shapiro [7] presented a more complex analysis of a flexible recording disk. The air was treated as an incompressible fluid with constant viscosity and negligible inertia. The flexible disk was modelled using linear membrane theory and the disk was assumed to derive its stiffness from the in-plane membrane forces of rotation. Solutions were obtained for steady and axisymmetric configuration.

Adams [8] examined the steady state solution of a disk spinning near a rigid wall. He included the effect of bending stiffness in his model for the disk and treated the fluid as incompressible. Carpino and Domoto [9] included the inertial effects in the modified Reynolds equation and determined the axisymmetric solution using the matched asymptotic expansions and a mixed numerical/perturbation procedure. Mahers and Adams [10] included von Kárman type non-linearities in their model and showed that for small gap sizes, the steady state displacement of the disk is not much different from the steady state displacement obtained using a linear plate model.

The effects of external excitations on the vibrations of spinning disks have also been considered in the literature. The external force can be a space fixed load or a moving load. The external force has often been used to model the effects of a read/write head in a computer memory disk.

Initial studies involved modelling the external force on a disk spinning in the absence of a surrounding medium. Benson and Bogy [11] approached the problem of a steady deflection of a flexible spinning disk due to a fixed transverse load within the context of the membrane theory. They observed that the membrane operator was singular. They concluded that the effect of bending stiffness, however small, has to be included. Cole and Benson [12] used an eigenfunction approach to identify the modes in transverse response of a flexible spinning disk subjected to a steady space-fixed transverse load.

Licari and King [13] studied the problem of elastohydrodynamic analysis of head-to-disk interface phenomena using a combination of finite element model for the disk and a finite difference model for the fluid. Effects of disk radius and disk thickness were investigated. Adams [14] investigated air flow between the disk and the base plate by means of two foundation parameters, stiffness and damping for each Fourier mode. The effect of using this new model and three other models on the point load solution and on the simulation of the disk-to-head interface was investigated.

Ono et al. [15] studied the mechanical interface between head and media in a flexible disk drive. Their model is a spinning disk partially supported by means of springs. They used Green's function for a spinning disk deflection to obtain the solutions, and concluded that the external stiffness had the effect of increasing the resonance speeds, whereas the external damping made the disk deflection asymmetric with respect to the applied force. Jiang et al. [16] examined the dynamic response of a read/write head floppy disk system subjected to axial excitation. The floppy disk was modelled as a spinning disk. The read/write head was modelled as a mass–spring system.

The stiffness of the air film in the cover was modelled as a set of uniform springs under the disk. They determined various resonance frequencies and forced response for the system.

Huang and Chiou [17] analyzed the vibrations of a spinning disk with moving head assembly where the magnetic head was modelled as a harmonically varying load traveling in the radial direction. The spinning disk response was solved for analytically using a Galerkin approach. They concluded that the moving speed of the load acts as a driving frequency and causes disk resonances at certain speeds. A constant load moving from the fixed end to the free end resulted in no oscillations, but it did cause oscillations when moving from the free end to the fixed end.

Disk-warpage also can have a significant effect on the vibratory response of a spinning disk. Wu and Adams [18], analyzed this effect for a flexible disk spinning in the presence of a thin air film while in contact with a point-head. They used a harmonic load to simulate the effect of a read/write head. In addition, they used a sinusoidal function to represent the axial excitation. From among the models they used for modelling the skew/warpage, they concluded that the effect of the skewed disk is to create a large deflection change and pitch angle variation. Carpino [19] employed a perturbation technique to study the effects of initial curvature on steady state configuration of the disk and compared results with experimental data obtained by Pelech and Shapiro [7]. He concluded that in cases where Young's modulus and the Poisson ratio have directional dependence, the directional variation in the properties will interact with the initial curvature.

Thus far, a brief review of the literature on the vibrations of spinning disks has been presented. The analysis becomes increasingly complex when the dynamic effects of fluid film are considered. The disk–fluid system can even undergo flutter instability and lead to self-excited oscillations which arise at certain wavenumbers above some rotational speeds of the disk. A review of the literature on flutter instability and ensuing oscillations can be found in a recent work of Naganathan et al. [20].

In the present work, a numerical approach is employed to study the forced response of a flexible spinning disc coupled to a thin air film. This direct numerical simulation gives insight into the response of the disk film combination without resorting to any approximation technique. More specifically, the effects of symmetric and constant as well as harmonically varying line loads on the vibratory response of a disk film system are studied. Thus, we consider a spinning flexible annular disk which is clamped at the inner end, is free at the outer end, and rotates about its vertical axis with a constant speed of Ω rad/s. The disk rotates close to a rigid base plate. The air flow between the disk and the base plate is modelled as an incompressible and laminar flow. The fluid flow and the disk deflection are coupled by means of the spacing and the pressure at the interface. The disk is modelled by a linear plate equation for a spinning disk. The equations governing the disk deflection and the fluid flow represent a set of coupled non-linear partial differential equations. These coupled non-linear evolution (time-dependent) equations are solved directly without subjecting them to linearizations or to any other approximation. In the numerical solution approach, the spatial derivatives are approximated by finite differences, where as the temporal solution is achieved by using Runge–Kutta algorithm. A direct numerical simulation tool is thus developed to solve the governing equations. This code has been recently used [20] to predict the existence of self-excited oscillations at sufficiently high wavenumbers and disk rotational speeds. It is here used to study the response of the disk–fluid system to time-independent as well as harmonically varying line loads. Thus, the effects of system design as well as forcing parameters can be evaluated.

2. Governing equations

2.1. Fluid equations

Consider an annular circular disk, clamped at its inner radius r_a, free at its outer radius r_b, and rotating at a constant angular velocity Ω. The lower surface of the disk is at a distance d from a rigid base plate, as shown in Fig. 1. The fluid flow between the disk and the base plate is modelled by simplifying the Navier–Stokes equations. The following basic assumptions regarding the flow are made: (1) the fluid is Newtonian; (2) the flow is laminar and incompressible; (3) the fluid viscosity is constant; (4) the thermal effects are negligible; (5) all fluid inertial forces, except for the centrifugal force, are negligible compared to the viscous forces; (6) the fluid film thickness is small compared to the diameter of the disk; thus, the pressure variation across the film thickness is negligible compared to variations in the plane perpendicular to the disk axis.

With these simplifying assumptions, the Navier–Stokes equations in the stationary frame can be written as

r-momentum:

$$-\rho_a \frac{v_\phi^2}{r} = -\frac{\partial P}{\partial r} + \mu \frac{\partial^2 v_r}{\partial z^2}, \tag{1}$$

ϕ-momentum:

$$0 = -\frac{1}{r}\frac{\partial P}{\partial \phi} + \mu \frac{\partial^2 v_\phi}{\partial z^2}, \tag{2}$$

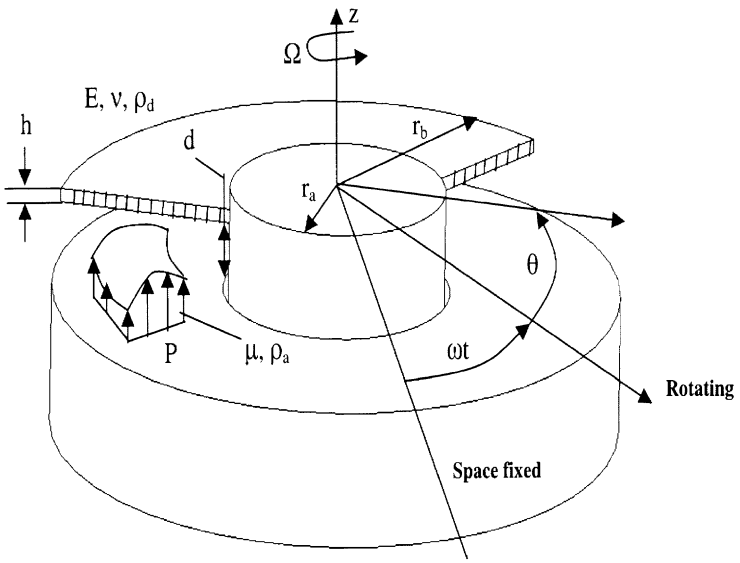

Fig. 1. Schematic representation of the disk–fluid model.

z-momentum:

$$0 = \frac{\partial P}{\partial z}, \tag{3}$$

where as, the *continuity equation* is given by

$$\frac{1}{r}\frac{\partial}{\partial r}(rv_r) + \frac{1}{r}\frac{\partial v_\phi}{\partial \phi} + \frac{\partial v_z}{\partial z} = 0, \tag{4}$$

where ρ_a is the density of the fluid and μ is its viscosity. The co-ordinate system is fixed at the radial center of the disk and coincides with the neutral plane of the disk in its undeformed position. The variable ϕ represents the stationary angular co-ordinate where as the variable θ denotes the angular co-ordinate rotating with the disk. The two co-ordinates are related by

$$\phi = \theta + \Omega t. \tag{5}$$

Associated with the four fluid equations, there are the boundary conditions. Three of these conditions are for no slip at the lower surface of the rotating disk. The remaining conditions are for no slip at the stationary disk boundary or the base plate. Note that at the base plate, $z = -(d + h/2)$. The boundary conditions for the fluid flow owing to the no slip condition then become

$$z = 0, \quad v_r = 0, \tag{6}$$

$$z = s(r, \phi, t), \quad v_r = 0, \tag{7}$$

$$z = 0, \quad v_\phi = 0, \tag{8}$$

$$z = s(r, \phi, t), \quad v_\phi = r\Omega, \tag{9}$$

$$z = 0, \quad v_z = 0, \tag{10}$$

$$z = s(r, \phi, t), \quad v_z = \frac{\partial s}{\partial t} + \Omega\frac{\partial s}{\partial \phi}. \tag{11}$$

Here, $s(r, \phi, t)$ represents the gap or the film thickness between the rotating disk and the stationary base plate. Now, integrating the ϕ-momentum and r-momentum equations, using the resulting expressions for v_ϕ and v_r into the continuity equation, and integrating it across the z direction, gives the equation

$$\frac{\partial}{\partial r}\left(\frac{rs^3}{\mu}\frac{\partial P}{\partial r}\right) + \frac{1}{r}\frac{\partial}{\partial \theta}\left(\frac{s^3}{\mu}\frac{\partial P}{\partial \theta}\right) = \left(\frac{3\rho_a\Omega^2}{10\mu}\right)\frac{\partial}{\partial r}\ (r^2 s^3)$$
$$- 6r\Omega\frac{\partial s}{\partial \theta} + 12r\frac{\partial s}{\partial t} - \frac{\rho_a}{10\mu^3}\frac{\partial}{\partial r}\left[\mu\Omega s^5\frac{\partial P}{\partial \theta} - \frac{3}{28}\frac{s^7}{r^2}\left(\frac{\partial P}{\partial \theta}\right)^2\right]. \tag{12}$$

This is the well-known Reynolds equation in the theory of lubrication for the pressure variation as a function of the radial distance r and the angle θ. The fluid pressure is assumed to be atmospheric at both the inner and the outer radius of the disk. The boundary conditions for

Eq. (12) are then

$$P(r_a) = P(r_b) = 0. \tag{13}$$

2.2. Disk equation

As already stated, the disk is of constant thickness, and is rotating with a constant angular velocity Ω. The following basic assumptions are made for the disk model: (1) the disk is made of an isotropic material; (2) the Youngs' modulus (E) and the Poissons' ratio (v) for the plate are constant; (3) the plate is linearly elastic so that Hooke's law holds; (4) for any point on the disk, the in-plane displacements (u, v) are much smaller than the transverse deflection (w), that is, $0 < u, v \ll w$; (5) transverse shear and rotatory inertia are ignored; (6) the transverse deflection (w) does not vary across the thickness of the disk, that is, $\varepsilon_{zz} = 0$; and (7) shear deflection is neglected, which implies that the normal shear strains are negligible, that is, $\varepsilon_{rz} = 0$, $\varepsilon_{\theta z} = 0$.

With these assumptions, the governing plate equation for a spinning disk, with both membrane and bending stiffness included, is given by

$$\frac{1}{r}\frac{\partial}{\partial r}\left(r\sigma_r \frac{\partial w}{\partial r}\right) + \frac{1}{r}\frac{\partial}{\partial \theta}\left(\sigma_\theta \frac{1}{r}\frac{\partial w}{\partial \theta}\right) - \frac{D}{h}\nabla^4 w + \frac{P}{h} + \frac{q}{h}\delta(r - r_i) = \rho_d \frac{\partial^2 w}{\partial t^2} + \frac{\mathrm{c}}{h}\frac{\partial w}{\partial t}. \tag{14}$$

Here, σ_r and σ_θ are the steady state stresses in the disk due to the centrifugal action of rotation, and they are given by

$$\sigma_r = \frac{\rho_d \Omega^2}{8}\left[(1+v)(r_a^2 + r_b^2\Gamma) - (3+v)r^2 + (1-v)\Gamma\frac{r_a^2 r_b^2}{r^2}\right],$$
$$\sigma_\theta = \frac{\rho_d \Omega^2}{8}\left[(1+v)(r_a^2 + r_b^2\Gamma) - (1+3v)r^2 - (1-v)\Gamma\frac{r_a^2 r_b^2}{r^2}\right], \tag{15}$$

where

$$\Gamma = \frac{-(1+v)r_a^2 + (3+v)r_b^2}{(1-v)r_a^2 + (1+v)r_b^2}.$$

Also, D is the bending stiffness of the disk, h is its thickness, P is the transverse pressure distribution at its surface due to the fluid, and ρ_d is the density of the disk material. Finally, q is a symmetric line load (force/length) located at the radius r_i. This load will be considered either as a constant or as harmonically varying in time.

Since Eq. (14) is a fourth order equation, four boundary conditions are needed. For the disk clamped at the inner radius, the displacement and the slope should vanish. Similarly, the shear and the bending moment vanish at the outer radius. Thus, the required boundary

conditions are

$$w(r_a,\theta,t)=0,\quad \left(\frac{\partial w}{\partial r}\right)_{(r=r_a,\theta,t)}=0,$$
$$M_{rr}(r_b,\theta,t)=-D\left[\frac{\partial^2 w}{\partial r^2}+\frac{v}{r}\left(\frac{\partial w}{\partial r}+\frac{1}{r}\frac{\partial^2 w}{\partial\theta^2}\right)\right]=0,$$
$$V_{rr}(r_b,\theta,t)=-D\left[\frac{\partial}{\partial r}(\nabla^2 w)+\frac{1-v}{r^2}\left(\frac{\partial^3 w}{\partial r\partial\theta^2}-\frac{1}{r}\frac{\partial^2 w}{\partial\theta^2}\right)\right]=0. \tag{16}$$

Eqs. (12)–(16) are the governing equations for the spinning flexible disk and the fluid flow between the disk and the rigid surface. This complete set of equations is now numerically solved without any further simplifications. As stated earlier, Naganathan et al. [20] developed a numerical technique to solve these equations starting from a specified initial condition. In the case of constant and harmonic external loads, the equations were integrated in time till the transients died down and a steady state was reached. Since the numerical technique is well documented, we do not give its details and focus more on the predicted responses for the disk–fluid system.

3. Forced oscillations

We consider the effect of an external harmonic load on the vibration of the disk spinning in the presence, and absence, of a surrounding medium. We also investigate the effect of the fluid film thickness on the oscillations of the disk. Only axisymmetric loads and responses near the lowest natural frequency of the disk are considered in this study.

3.1. Response to a steady line load

First consider the steady state deflection of a disk under the influence of a constant load. The position and the magnitude of the load are varied to observe the effects of the load magnitude and location. The parameter set for the numerical studies used is: $r_a=10$ mm, $r_b=140$ mm, $\rho_a=1.23$ kg/m^3, $\rho_d=1100$ kg/m^3, $E=1.47\times10^8$ N/m^2, $\mu=18.6\times10^{-6}$ Ns/m^2, $d=1.0$ mm, $h=38\times10^{-6}$ m and $v=0.3$. Various cases are considered in which the location and magnitude of the line load are varied.

Case i. $r_i=51.0$ mm, $\Omega=1000$ rpm: The magnitudes of the load q used for steady state axisymmetric response are -5, -10, -30, -50, -75 and -100 N/m. The steady state deflection and pressure variations are shown in Figs. 2 and 3.

Case ii. $r_i=91.0$ mm, $\Omega=1000$ rpm: The same magnitudes of the load, -5, -10, -30, -50, -75 and -100 N/m, are used here. Thus, the only difference with Case i above is in the location of the circular line load. The steady state deflection and pressure variations are shown in Figs. 4 and 5.

Case iii. $r_i=131.0$ mm, $\Omega=1000$ rpm: Again, the same magnitudes of the load q are used. The load is applied very near the outer periphery of the disk. The steady state deflection and pressure variations are shown in Figs. 6 and 7.

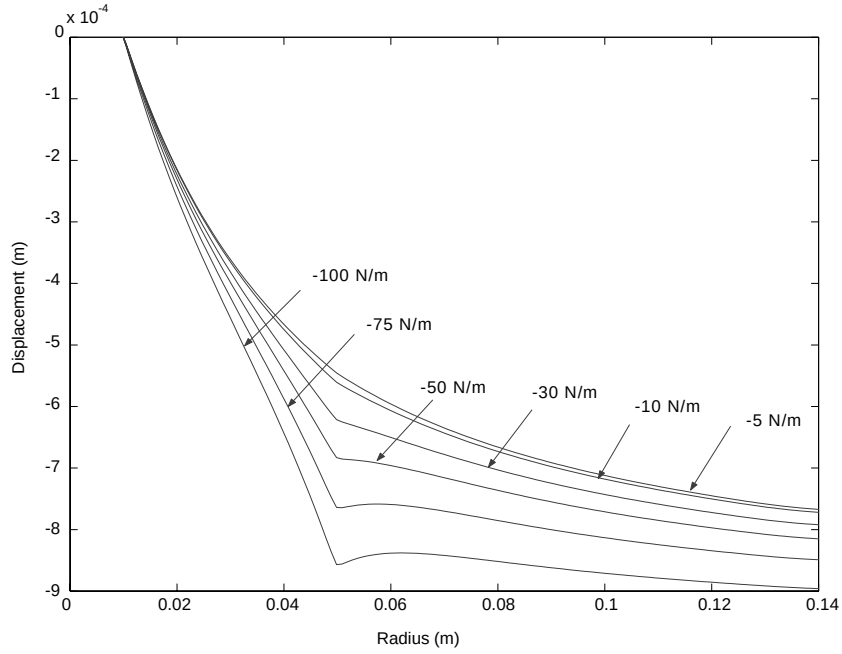

Fig. 2. Steady state deflection of a disk for line loads of different magnitude at $r_i = 51$ mm. The parameters are: $r_a = 10$ mm, $r_b = 140$ mm, $\rho_a = 1.23$ kg/m^3, $\rho_d = 1100$ kg/m^3, $E = 1.47 \times 10^8$ N/m^2, $\mu = 18.6 \times 10^{-6}$ Ns/m^2, $d = 1.0$ mm, $h = 38 \times 10^{-6}$ m, $v = 0.3$ and $\Omega = 1000$ rpm.

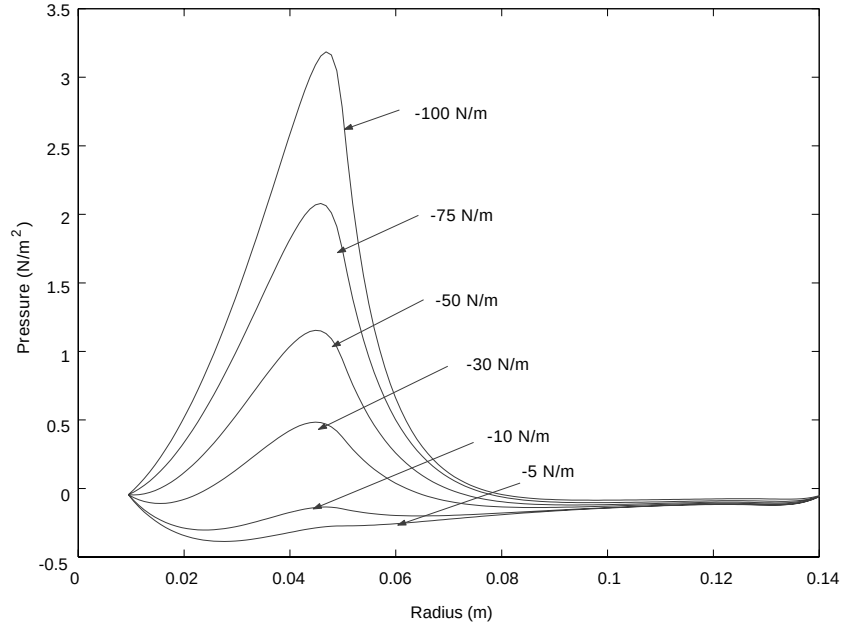

Fig. 3. Steady state pressure field for line loads of different magnitude at $r_i = 51$ mm. The parameters are: $r_a = 10$ mm, $r_b = 140$ mm, $\rho_a = 1.23$ kg/m^3, $\rho_d = 1100$ kg/m^3, $E = 1.47 \times 10^8$ N/m^2, $\mu = 18.6 \times 10^{-6}$ Ns/m^2, $d = 1.0$ mm, $h = 38 \times 10^{-6}$ m, $v = 0.3$ and $\Omega = 1000$ rpm.

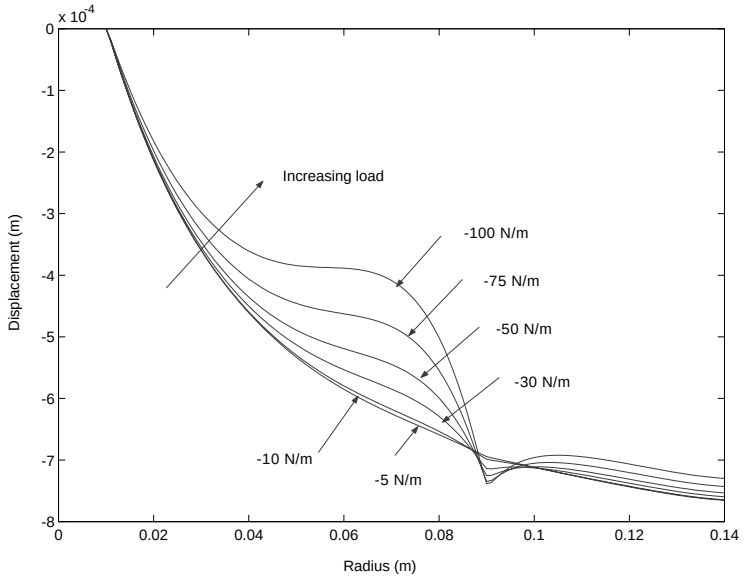

Fig. 4. Steady state deflection of a disk for line loads of different magnitude at $r_i = 91$ mm. The parameters are: $r_a = 10$ mm, $r_b = 140$ mm, $\rho_a = 1.23$ kg/m^3, $\rho_d = 1100$ kg/m^3, $E = 1.47 \times 10^8$ N/m^2, $\mu = 18.6 \times 10^{-6}$ Ns/m^2, $d = 1.0$ mm, $h = 38 \times 10^{-6}$ m, $v = 0.3$ and $\Omega = 1000$ rpm.

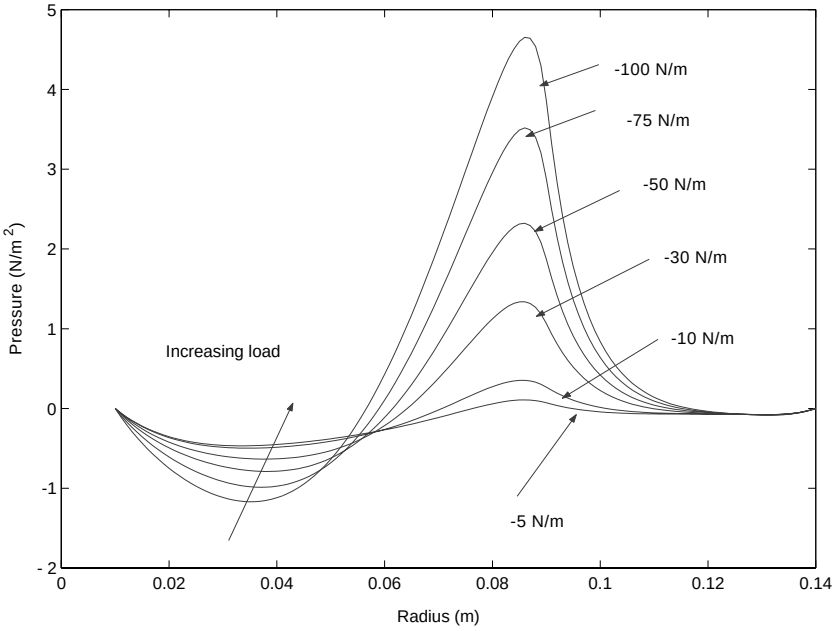

Fig. 5. Steady state pressure field for line loads of different magnitude at $r_i = 91$ mm. The parameters are: $r_a = 10$ mm, $r_b = 140$ mm, $\rho_a = 1.23$ kg/m^3, $\rho_d = 1100$ kg/m^3, $E = 1.47 \times 10^8$ N/m^2, $\mu = 18.6 \times 10^{-6}$ Ns/m^2, $d = 1.0$ mm, $h = 38 \times 10^{-6}$ m, $v = 0.3$ and $\Omega = 1000$ rpm.

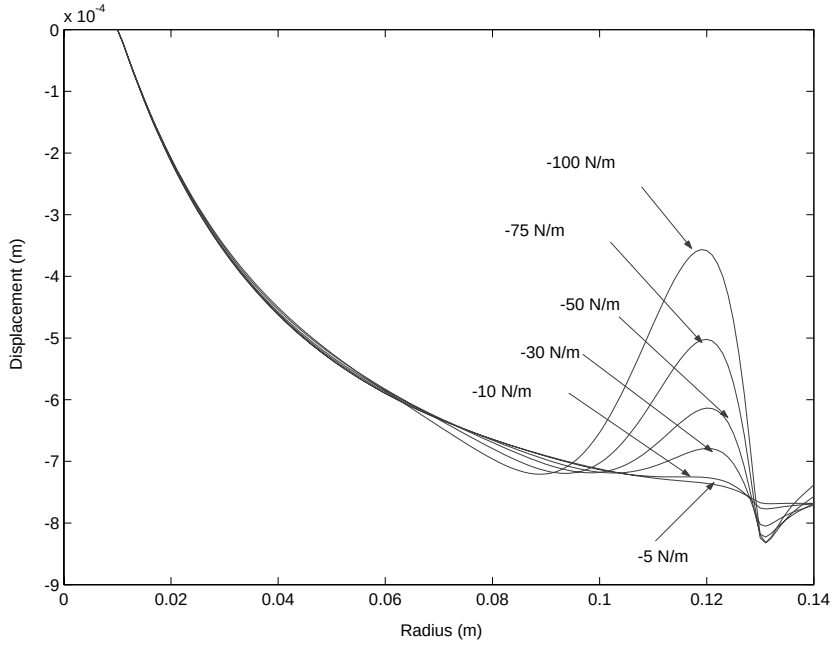

Fig. 6. Steady state deflection of a disk for line loads of different magnitude at $r_i = 131$ mm. The parameters are: $r_a = 10$ mm, $r_b = 140$ mm, $\rho_a = 1.23$ kg/m^3, $\rho_d = 1100$ kg/m^3, $E = 1.47 \times 10^8$ N/m^2, $\mu = 18.6 \times 10^{-6}$ Ns/m^2, $d = 1.0$ mm, $h = 38 \times 10^{-6}$ m, $v = 0.3$ and $\Omega = 1000$ rpm.

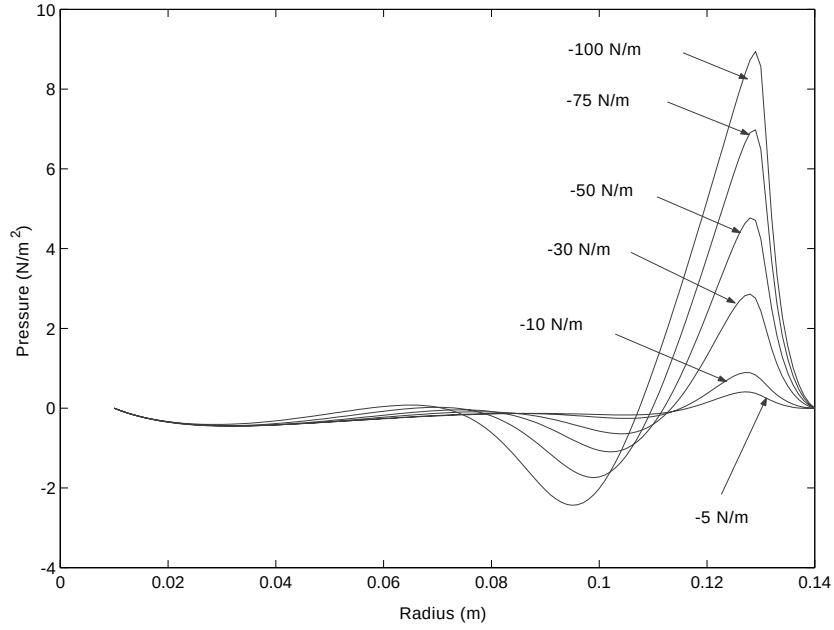

Fig. 7. Steady state pressure field for line loads of different magnitude at $r_i = 131$ mm. The parameters are: $r_a = 10$ mm, $r_b = 140$ mm, $\rho_a = 1.23$ kg/m^3, $\rho_d = 1100$ kg/m^3, $E = 1.47 \times 10^8$ N/m^2, $\mu = 18.6 \times 10^{-6}$ Ns/m^2, $d = 1.0$ mm, $h = 38 \times 10^{-6}$ m, $v = 0.3$ and $\Omega = 1000$ rpm.

It is seen that the deflections under the load are higher for the case when the load is applied at $r_i = 51$ mm, than at $r_i = 131$ mm. This is due to the smaller film thickness at the outer radius and hence the associated higher stiffness. This helps in supporting the load at the outer ends of the disk. However, it can be noted from the plots of the pressure field in Figs. 3, 5 and 7, that a small change in displacement under the load causes the pressure in the upstream to increase. Thus, as the load increases, the fluid pressure builds up to support the load. Another point to note is that when the load is applied close to the fixed center of the disk ($r_i = 51$ mm), the deflection of the disk increases monotonically with the load as shown in Fig. 2. This is, however not true when the load line moves close to the outer free end of the disk as seen in Fig. 6.

3.2. Forced harmonic response in the absence of the fluid film

First consider the resonant response of a disk in the absence of the fluid. A harmonic line load is applied circumferentially along a line of constant radius r_i. The response of the spinning plate is then governed by Eq. (14) with $P = 0$. The parameter set used is the same as the one given in the previous section. The harmonic load is assumed to be of the form

$$q = q_0 \cos(\tilde{\omega} t), \tag{17}$$

where q_0 chosen for simulations is -4 N/m, and the line load is located at $r_i = 91$ mm. Approximations to the lowest few natural frequencies of a spinning disk for axisymmetric modes,

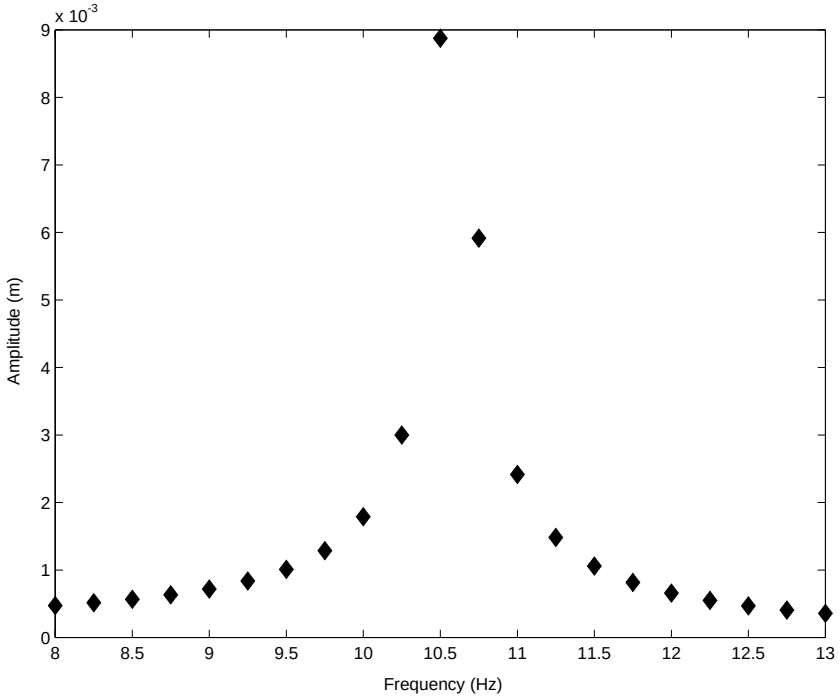

Fig. 8. Amplitude at the point $r_i = 91$ mm on the disk spinning in the absence of a surrounding medium, due to a harmonic load. The parameters are: $r_a = 10$ mm, $r_b = 140$ mm, $\rho_d = 1100$ kg/m^3, $E = 1.47 \times 10^8$ N/m^2, $h = 38 \times 10^{-6}$ m, $v = 0.3$, $q_0 = -4$ N/m and $\Omega = 1000$ rpm.

for the parameter set chosen, are found using the Rayleigh–Ritz technique. These natural frequencies are used in identifying the excitation frequencies to be provided in the numerical code in order to excite resonant behavior. A small damping term has also been intentionally introduced into the governing equation (14) in order to limit the response when the excitation frequency is near one of the natural frequencies. The coefficient c is chosen to be equal to 10% of the critical damping coefficient (c_c). The critical damping is found utilizing the natural frequencies obtained by the Rayleigh–Ritz technique. The simulations are performed for various values of the excitation frequency $\tilde{\omega}$ in the range of 8–13 Hz, and the amplitude of the steady state harmonic response is plotted as a function of the frequency (see Fig. 8). It is seen that the amplitude of response, plotted for the point (or circle) of application, rises very sharply close to resonance and decays as the exciting frequency moves far away from the first natural frequency. Thus, as is expected, the amplitude of vibration of a spinning disk in the absence of the surrounding medium, can be high for low damping.

3.3. Forced harmonic response in the presence of the fluid film

We now consider the effect of the fluid film on the steady state harmonic response of the spinning disk.

The simulations were performed for frequencies of excitations ($\tilde{\omega}$) in the range of 1 to 13 Hz. The amplitude of the steady state periodic response at the point of application of the harmonic

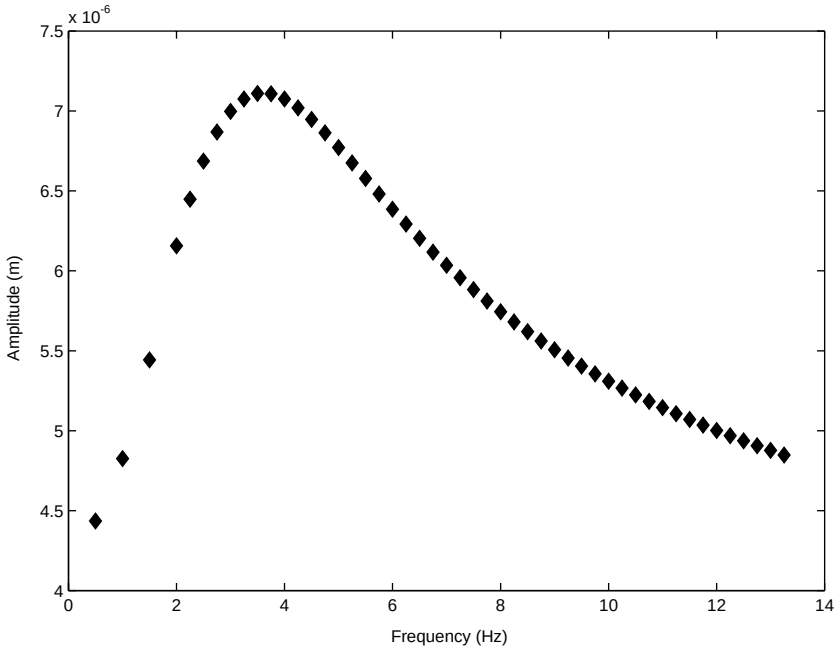

Fig. 9. Amplitude at the point $r_i = 91$ mm on the disk spinning in the presence of a surrounding medium, due to harmonic load. The parameters are: $r_a = 10$ mm, $r_b = 140$ mm, $\rho_a = 1.23$ kg/m^3, $\rho_d = 1100$ kg/m^3, $E = 1.47 \times 10^8$ N/m^2, $\mu = 18.6 \times 10^{-6}$ Ns/m^2, $d = 1.0$ mm, $h = 38 \times 10^{-6}$ m, $v = 0.3$, $q_0 = -4$ N/m and $\Omega = 1000$ rpm.

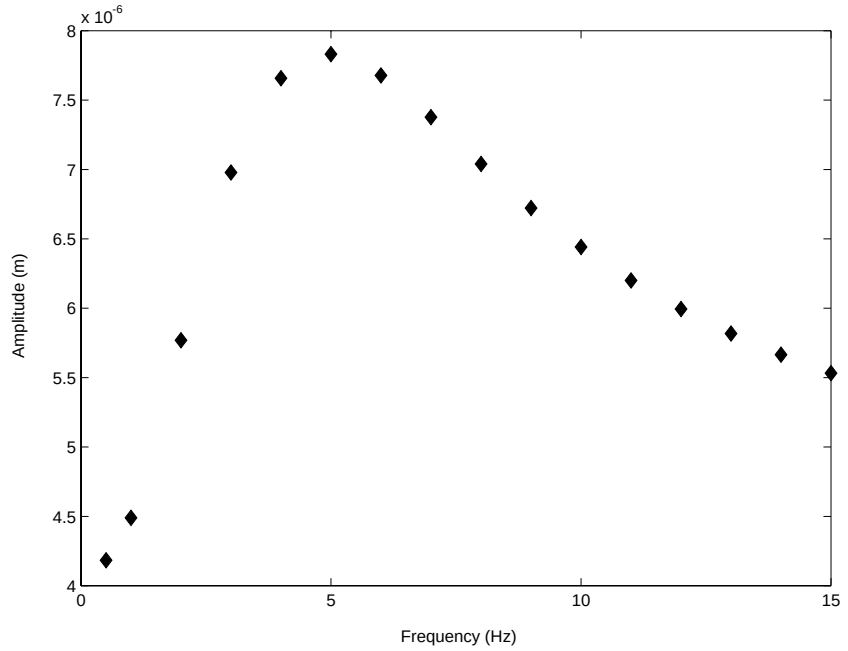

Fig. 10. Amplitude of the point $r_i = 91$ mm on the disk spinning in the presence of a surrounding medium, due to a harmonic load. The parameters are: $r_a = 10$ mm, $r_b = 140$ mm, $\rho_a = 1.23$ kg/m^3, $\rho_d = 1100$ kg/m^3, $E = 1.47 \times 10^8$ N/m^2, $\mu = 18.6 \times 10^{-6}$ Ns/m^2, $d = 1.2$ mm, $h = 38 \times 10^{-6}$ m, $v = 0.3$, $q_0 = -4$ N/m and $\Omega = 1000$ rpm.

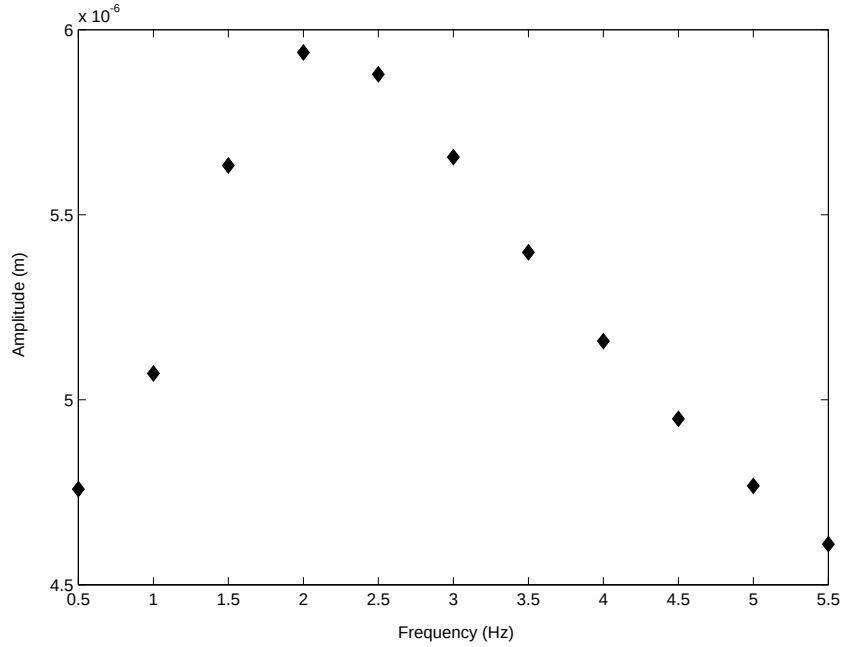

Fig. 11. Amplitude of the point $r_i = 91$ mm on the disk spinning in the presence of a surrounding medium, due to a harmonic load. The parameters are: $r_a = 10$ mm, $r_b = 140$ mm, $\rho_a = 1.23$ kg/m^3, $\rho_d = 1100$ kg/m^3, $E = 1.47 \times 10^8$ N/m^2, $\mu = 18.6 \times 10^{-6}$ Ns/m^2, $d = 0.7$ mm, $h = 38 \times 10^{-6}$ m, $v = 0.3$, $q_0 = -4$ N/m and $\Omega = 1000$ rpm.

load ($r = 91$ mm), for a system with film thickness $d = 1.0$ mm, is shown in Fig. 9. Compared to the disk response without the fluid, two effects can be noted immediately. First, the resonant, or maximum, response frequency is reduced drastically. Furthermore, the maximum amplitude of vibration has decreased considerably when the effect of the fluid is included in the model. The fluid provides damping, which helps in reducing the amplitude of vibration.

When the air or film gap size is small, the air adds considerable inertia to the disk due to slender aspect ratio of the air bearing. Small accelerations of the disk result in large accelerations in the fluid. The added inertia also reduces the resonant frequency. Thus, it is seen that the surrounding fluid plays an important role in controlling the vibrations of the spinning disk.

In order to evaluate the damping, inertial and stiffening effects of the fluid film, response curves are generated for various gap sizes. The gap size is increased to $d = 1.2$ mm with all the other parameters being the same. The steady state amplitude–response curve is shown in Fig. 10. It is seen that the resonance frequency has shifted to a higher frequency. The peak amplitude of response has also increased compared to the case of $d = 1.0$ mm. The ability of the fluid to support the load has decreased as the gap size has increased.

Similar response curves were also generated for gap sizes $d = 0.7$, 1.5 and 2.0 mm, and the results are shown in Figs. 11–13. It is seen in all the cases that the amplitude of vibration increases as the gap size increases. This is also accompanied by an increase in resonant response frequency. Furthermore, the response curves get flattened out as the gap size increases and the large

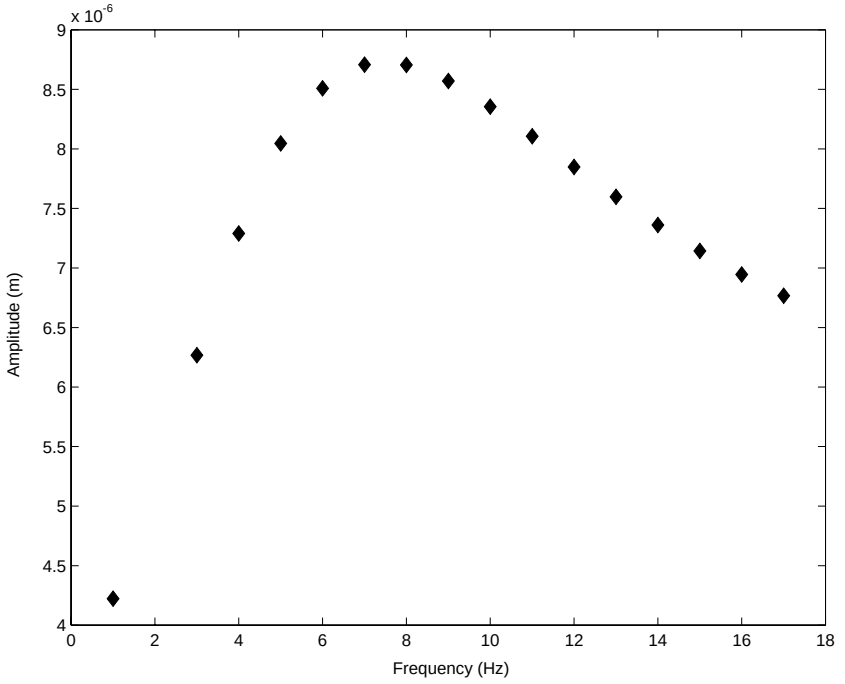

Fig. 12. Amplitude of the point $r_i = 91$ mm on the disk spinning in the presence of a surrounding medium, due to a harmonic load. The parameters are: $r_a = 10$ mm, $r_b = 140$ mm, $\rho_a = 1.23$ kg/m^3, $\rho_d = 1100$ kg/m^3, $E = 1.47 \times 10^8$ N/m^2, $\mu = 18.6 \times 10^{-6}$ Ns/m^2, $d = 1.5$ mm, $h = 38 \times 10^{-6}$ m, $v = 0.3$, $q_0 = -4$ N/m and $\Omega = 1000$ rpm.

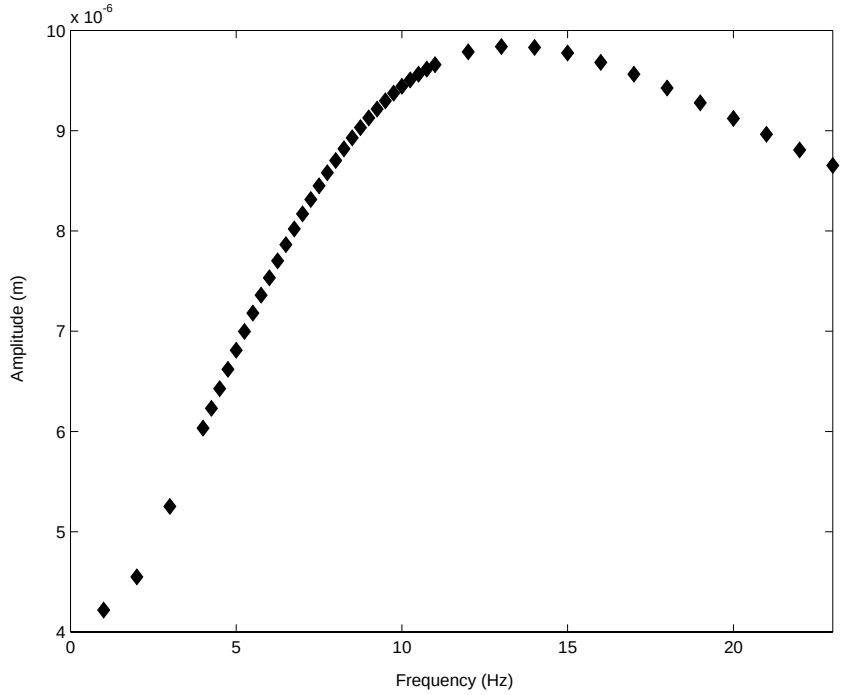

Fig. 13. Amplitude at the point $r_i = 91$ mm on the disk spinning in the presence of a surrounding medium, due to a harmonic load. The parameters are: $r_a = 10$ mm, $r_b = 140$ mm, $\rho_a = 1.23$ kg/m^3, $\rho_d = 1100$ kg/m^3, $E = 1.47 \times 10^8$ N/m^2, $\mu = 18.6 \times 10^{-6}$ Ns/m^2, $d = 2.0$ mm, $h = 38 \times 10^{-6}$ m, $v = 0.3$, $q_0 = -4$ N/m and $\Omega = 1000$ rpm.

amplitude response exists over a wider frequency interval. Thus, the fluid helps in controlling the amplitude of vibration in the presence of an external harmonic loading on the disk. This is in addition to the enhanced stability achieved by spinning a disk close to the base plate. As the gap size is increased, the tendency for the fluid to support the load decreases. Due to this the disk gets deflected closer to the base plate under the point of application of the load which in turn increases the pressurization. This pressurization might be creating a local stiffening effect due to which the resonant frequency is increased.

4. Summary

The steady state axisymmetric deflection of a spinning disk under the influence of a constant line load for various locations and magnitude of the load has been studied. It is seen that as the load magnitude increases, the fluid pressure builds up to the level required to support the load. In the case of a disk spinning in the absence of a surrounding medium, the amplitude of response of the disk increases considerably when the excitation frequency of a harmonic load is close to the natural frequency of the disk. When the effect of the surrounding medium is introduced, the resonant response frequency as well as the maximum amplitude of response are seen to decrease

with a decrease in the film thickness. This is in addition to the dampening effect expected due to the presence of the spinning viscous fluid.

References

[1] H. Lamb, R.V. Southwell, The vibrations of a spinning disk, Proceedings of the Royal Society of London 99 (1921) 272–280.
[2] R.V. Southwell, On the free transverse vibrations of a uniform circular disk clamped at its center and on the effects of rotation, Proceedings of the Royal Society of London 101 (1922) 133–153.
[3] J. Prescott, Applied Elasticity, Dover Publication, New York, 1946.
[4] J. Simmonds, The transverse vibrations of a flat spinning membrane, Journal of the Aeronautical Sciences 29 (1962) 16–18.
[5] W. Eversman, R.O. Dodson Jr., Free vibration of a centrally clamped spinning circular disk, American Institute of Aeronautics and Astronautics Journal 7 (10) (1969) 2010–2012.
[6] R. Pearson, The development of the flexible-disk magnetic recorder, Proceedings of the IRE 49 (1961) 164–174.
[7] I. Pelech, A.H. Shapiro, Flexible disk rotating on a gas film next to a wall, American Society of Mechanical Engineers Journal of Applied Mechanics 31 (1964) 577–584.
[8] G.G. Adams, Analysis of the flexible disk/head interface, Journal of Lubrication Technology 102 (1980) 86–90.
[9] M. Carpino, G.A. Domoto, Investigation of a flexible disk rotating near a rigid surface, American Society of Mechanical Engineers Journal of Tribology 110 (1988) 664–669.
[10] J.F. Maher, G.G. Adams, Effect of displacement dependent membrane stresses on the axi-symmetric configuration of a spinning flexible disk, Tribology Transactions 34 (1991) 597–603.
[11] R.C. Benson, D.B. Bogy, Deflection of a very flexible spinning disk due to a stationary transverse load, American Society of Mechanical Engineers Journal of Applied Mechanics 45 (1978) 636–642.
[12] K.A. Cole, R.C. Benson, A fast eigenfunction approach for computing spinning disk deflection, American Society of Mechanical Engineers Journal of Applied Mechanics 55 (1988) 453–457.
[13] J.P. Licari, F.K. King, Elastohydrodynamic analysis of head to flexible disk interface, American Society of Mechanical Engineers Journal of Applied Mechanics 48 (1981) 763–768.
[14] G.G. Adams, The point-load solution and simulation of a flexible spinning disk using various disk-to-baseplate air-flow models, Tribology Transactions 36 (3) (1993) 470–476.
[15] K. Ono, T. Maeno, T. Ebihara, Study of mechanical interface between head and media in flexible disk drive, Bulletin of JSME 29 (1986) 3109–3115.
[16] Z.W. Jiang, S. Chonan, H. Abe, Dynamic response of a read/write head floppy disk system subjected to axial excitation, American Society of Mechanical Engineers Journal of Vibration and Acoustics 112 (1990) 53–58.
[17] S.C. Huang, W.J. Chiou, Modeling and vibration analysis of spinning-disk and moving-head assembly in computer storage system, American Society of Mechanical Engineers Journal of Vibration and Acoustics 119 (1997) 185–191.
[18] W. Wu, G.G. Adams, The effect of disk warpage/skew on the deflection and vibration of a flexible disk spinning above a baseplate and in contact with a point-head, American Society of Mechanical Engineers Journal of Tribology 119 (1997) 64–70.
[19] M. Carpino, The effect of initial curvature in a flexible disk rotating near a flat plate, American Society of Mechanical Engineers Journal of Tribology 113 (1991) 355–360.
[20] G. Naganathan, A.K. Bajaj, S. Ramadhyani, Numerical simulations of flutter instability of a flexible disk rotating close to a rigid wall, Journal of Vibration and Control 9 (2003) 95–118.